

Influence of Substitution on the Supramolecular Chemistry of Cycloparaphenylene-Fullerene Complexes

Daniel Kohrs^{+, [a, b]}, Jannis Volkmann^{+, [a, b]} and Hermann A. Wegner^{*[a, b]}

We present a comprehensive host-guest study of four substituted and unsubstituted [10]cycloparaphenylenes with the fullerenes C₆₀ and C₇₀. Within this study, the influence on the complexation behavior was investigated experimentally and computationally. Due to the increased steric demand the substitution on the nanohoop results in an energetic penalty, which could be partially compensated by additional substituent-fullerene interactions. These attractive interactions are intensified in the C₇₀ complexes and with an increased degree

of substitution. For the computational investigation conformer ensembles were taken into account, providing reliable structures with Boltzmann weighted energies. An analysis of the noncovalent interactions elucidated the origin of the enhanced substituent-C₇₀ interaction. The ellipsoid fullerene C₇₀ can be considered as a π -extended version of C₆₀, which is able to increase the attractive van der Waals interactions within these supramolecular complexes.

Introduction

Interactions between not covalently bound molecules are omnipresent, reaching from solvation to protein folding and beyond. In the field of π -conjugated (nano)carbons, π - π interactions play a crucial role between the nanocarbons, as well as in their solvation. The term π - π interaction joins a library of interactions consisting of quadrupole interactions,^[1] electrostatic interactions as well as London dispersion among others.^[2]

A prime example among these interactions is the π -stacking of two graphene layers within graphite. Here, the lattices stack in a displaced manner with an interlayer distance of 3.40 Å.^[3] Wrapped-up graphene sheets, carbon nanotubes (CNT), have an increased and decreased electron density on the concave and convex site, respectively, which makes them suitable candidates to host fullerenes in their electron-rich cavity. The shortest repeatable cut-out of an armchair CNT is a [n]cycloparaphenylene ([n]CPP) which can thus be seen as the perfect model substrate for single-walled CNTs. After years of throwbacks on the synthetic odyssey towards these strained polyaromatic hydrocarbons,^[4] three main strategies were developed to form this class of curved compounds.^[5] Having these

strategies established, it was possible to investigate a variety of different sized CPPs for which [10]CPP revealed superior supramolecular properties regarding complexation with fullerenes. The [10]CPP@C₆₀ complex, for instance, has an exceptional association constant of around 10⁷ M⁻¹ in toluene.^[6] In this complex the distance between the nanohoop and the fullerene coincides with the interlayer distance in graphite. A similar strategy was applied by our group for the stabilization of the azafullerenyl radical C₅₉N[•],^[7] as well as by others for the synthesis of a rotaxane^[8] or the complexation of charge-delocalized endofullerenes.^[9] In case of bisazafullerene (C₅₉N)₂, the fullerene dimer can be encapsulated by two [10]CPPs, whereat the first complexation promotes the second by additional London dispersion forces.^[10]

While a substituted *para*-phenylene unit within a CPP influences the association constant due to a decreased diameter and conjugation originating from the larger dihedral angle of the substituted core unit with the adjacent phenylenes, additional interactions – such as London dispersion – can positively contribute to the association (Figure 1). Recently, we investigated these additional interactions in complexes consisting of a di *tert*-butyl ester functionalized [10]CPP as a host unit encapsulating different methanofullerenes, functionalized with branched as well as linear alkyl chains.^[11] In all cases, the

[a] D. Kohrs,⁺ J. Volkmann,⁺ Prof. Dr. H. A. Wegner
Institute of Organic Chemistry
Justus Liebig University Giessen
Heinrich-Buff-Ring 17, 35392 Giessen (Germany)
E-mail: Hermann.A.Wegner@org.chemie.uni-giessen.de

[b] D. Kohrs,⁺ J. Volkmann,⁺ Prof. Dr. H. A. Wegner
Center for Materials research (ZfM/LaMa)
Justus Liebig University Giessen
Heinrich-Buff-Ring 16, 35392 Giessen (Germany)

[†] These authors contributed equally to this work.

Supporting information for this article is available on the WWW under <https://doi.org/10.1002/ejoc.202300575>

© 2023 The Authors. European Journal of Organic Chemistry published by Wiley-VCH GmbH. This is an open access article under the terms of the Creative Commons Attribution Non-Commercial License, which permits use, distribution and reproduction in any medium, provided the original work is properly cited and is not used for commercial purposes.

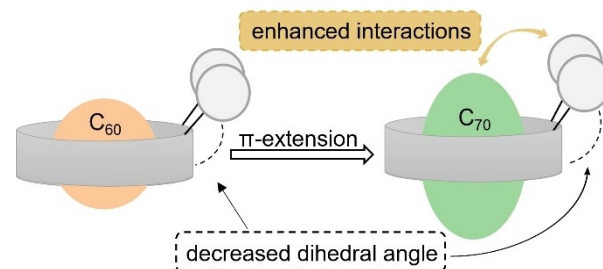


Figure 1. Schematic representation of the proposed enhanced interaction between the π -extended fullerene C₇₀ and the substituents on the CPP.

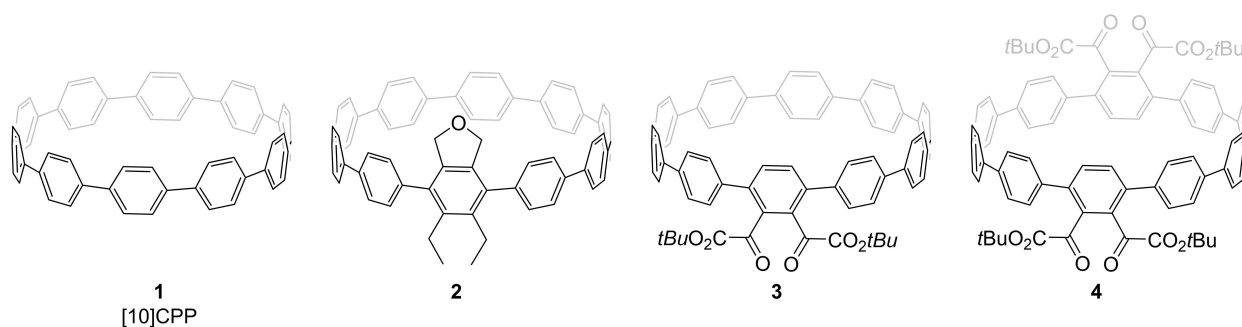


Figure 2. CPPs applied within this study.

attractive interactions dominated, with the dispersion donors *n*-butyl and 1-adamantyl showing the strongest effect. To get an in-depth understanding of the substitution effects in CPP-fullerene complexes, we have herein conducted fluorescence quenching experiments with the previously reported di- and tetra-*tert*-butyl ester functionalized [10]CPPs 3 and 4, as well as the diethyl phthalane incorporated [10]CPP 2, in comparison to the parent [10]CPP 1 (Figure 2). The fullerenes C_{60} and C_{70} were employed as guest molecules and the impact of the different shapes of the fullerenes on the association behavior with the substituted nano hoops were investigated experimentally as well as by theoretical calculations.

Results and Discussion

Experimental details

The substituted CPPs – di- and tetra-*tert*-butyl ester functionalized [10]CPPs 3 and 4, as well as diethyl phthalane incorporated [10]CPP 2 – were synthesized according to previously published syntheses,^[12,13] following a similar strategy relying on a combination of a [2+2+2] cycloaddition for the introduction of substituents and a cross-coupling reaction for the selective formation of the 10-membered ring.^[14] The unsubstituted [10]CPP 1 was synthesized following a synthesis reported by Jasti and coworkers.^[15]

For the determination of the association constants, trifold fluorescence quenching experiments were conducted in toluene and the thus obtained standard deviation was employed for the errors. While the concentration of the emitting host (CPP) was kept constant, the guest concentration was varied, and the quenching of the fluorescence was followed. The data were evaluated by non-linear regression utilizing the online tool “bindfit” by Thordarson.^[16] For the determination of the stoichiometry, association mode and association constant the corresponding recommendations by Thordarson were followed. Even though the association constant of parent [10]CPP with C_{70} is literature known, we repeated the experiments to rule out systematic deviations originating from different experimental setups.

Association Constants

The association constants and energies of the different C_{60} and C_{70} /CPP-complexes are summarized in Table 1 and Figure 3. In general, the association drops upon substitution of the nano hoop which is in accordance with our earlier results for methanofullerenes.^[11] This trend can be rationalized by the increased dihedral angle between the substituted aromatic ring and the adjacent ones which effectively reduces the inner diameter and thus the cavity available for the fullerene (Figure 1). The dihedral angle has to be reduced upon complex-

Table 1. Summary of the binding energies used for Figure 1 as well as the corresponding association energies for the investigated complexes with the standard deviations after trifold determination. The values 1@ C_{60} and 3@ C_{60} are taken from ref. [11].

Host	Guest	$K_{\text{bind}}/\text{M}^{-1}$	$\Delta G_{\text{bind,measur}}/\text{kJ/mol}$
1	C_{60}	$7.1 \pm 0.1 \cdot 10^6$	-39.09 ± 0.05
	C_{70}	$4.7 \pm 0.2 \cdot 10^5$	-32.4 ± 0.1
2	C_{60}	$1.15 \pm 0.08 \cdot 10^5$	-28.9 ± 0.2
	C_{70}	$3.75 \pm 0.08 \cdot 10^4$	-26.10 ± 0.06
3	C_{60}	$7.5 \pm 0.3 \cdot 10^5$	-33.5 ± 0.1
	C_{70}	$7.7 \pm 0.3 \cdot 10^4$	-27.88 ± 0.08
4	C_{60}	$1.0 \pm 0.1 \cdot 10^5$	-28.6 ± 0.3
	C_{70}	$4.1 \pm 0.7 \cdot 10^4$	-26.3 ± 0.5

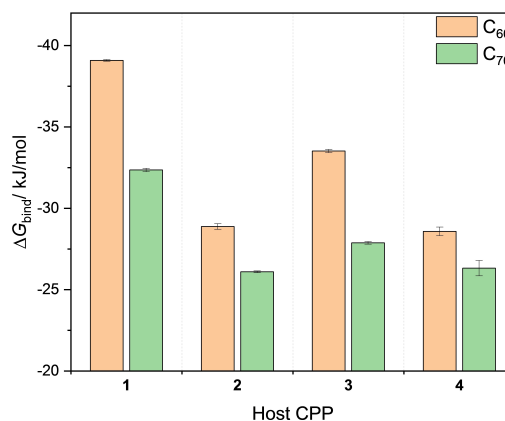


Figure 3. Association energies of the investigated nano hoop molecules with C_{60} as well as C_{70} .

ation – a penalty which has to be paid with association energy. Additionally, this trend amplifies with an increasing degree of substitution and contributes to both, the association with C_{60} and C_{70} . For the two fourfold-substituted derivatives **2** and **4** the values are very similar, indicating a weak influence of the nature of the substituents in the investigated cases.

To analyze the interactions, the binding energies were normalized to the energies of the parent complexes $1@C_{60}$ and $1@C_{70}$, respectively (Figure 4, orange and green bars). Thus, the sum of energetic penalty arising from a decreased effective inner diameter and attractive non-covalent interactions can be rationalized. In all cases the association energy is reduced by 10%–30%, correlating to a reduction of the association constant by about one order of magnitude, given the exponential relation between association constant and its energy (Supporting Information, EQ S1). However, it is clearly visible that the relative drop in the association energy is stronger for C_{60} among all substituted CPPs. This fact is supported by the $\Delta\Delta G_{\text{bind,rel}}$ values calculated with Equation (1). This value emphasizes the differences between the C_{60} and C_{70} complexes. A value of 100% indicates no influence of the nature of fullerene, while a value < 100% indicates a stabilization of C_{70} over C_{60} , and *vice versa*. In all three cases $\Delta\Delta G_{\text{bind,rel}}$ is < 100%, showing the stabilizing effect of C_{70} over C_{60} (Figure 4, purple bar).

$$\Delta\Delta G_{\text{bind,rel}} = \frac{\Delta G_{\text{bind,rel}}(C_{60})}{\Delta G_{\text{bind,rel}}(C_{70})} \quad (1)$$

While the lower sphericity of C_{70} leads to a weaker interaction with the nanoring, even in the parent complexes, it bears an additional surface for further interactions in the substituted cases which is the main reason for the smaller penalty paid upon substitution.

C_{70} can be seen as a π -extended C_{60} . The attractive CH- π and lone pair- π interactions of the CPP substituents with the convex surface of the fullerene improve the association and lead to a smaller decrease in association compared to C_{60} . This

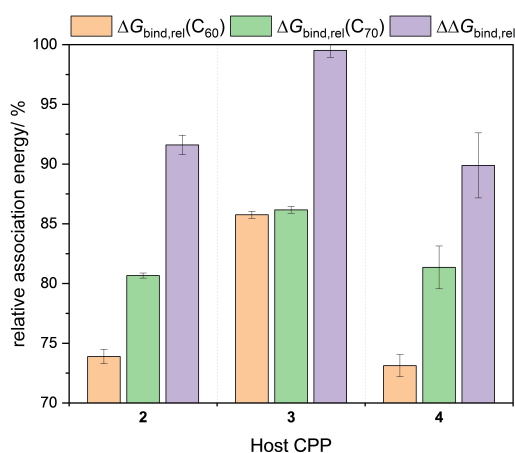


Figure 4. Relative association energies normalized on the association energy of the parent complex with [10]CPP.

assumption is supported by the fact that this trend is enhanced upon a higher degree of substitution, possessing thus more interacting entities.

For the twofold substituted CPP **3** the value is very close to 100% and hence, there is only a marginal difference between the fullerenes, which indicates interactions with C_{60} and C_{70} to have a similar quantity. On the other hand, the fourfold substituted CPPs **2** and **4** exhibit a value of around 90%, which could be explained by a similar contact surface between substituents and curved fullerene surface.

Theoretical Investigation

Computational details

The computational details are briefly described in the following while a more exhaustive description can be found in the supplementary information. All density functional theory (DFT) calculations were executed with the software package orca (version 5.0.4).^[17] The RIJCOSX approximations,^[18–21] utilizing the auxiliary basis set def2-J were used as default. To get reliable geometries and energies, the hosts, as well as the complexes were subjected to the conformer-rotamer ensemble sampling tool (CREST) by Grimme.^[22] The obtained ensemble was submitted to the command line energetic sorting of conformer rotamer ensembles (CENSO) workflow,^[23] obtaining a narrowed ensemble with geometries and energies on a DFT level. The geometries were obtained by the r2SCAN-3c/mDZ method,^[24] accompanied with the solvation model based on molecular electron density (SMD^[25]) energy and the modified rigid rotator harmonic oscillator (mRRHO^[26]) approach with Grimme's extended tight binding method (xtB-gfn2)^[27] based thermodynamic correction. The single point energies were obtained with the hybrid DFT method PBE0 with D4 dispersion correction,^{[19,20][18,28]} combined with the triple- ζ def2-TZVP basis set,^[19] in conjunction with the SMD solvent model and the mRRHO(gfn2) approximation for the thermodynamic contribution. The final ensemble represents 99% of the Boltzmann distribution among all observed conformers. Utilizing the Boltzmann weighted energies for the CPPs and complexes, the energy contributions of the present conformers were taken into account. The non-covalent interaction (NCI) in the supramolecular complexes were calculated with the NCIPLOT 4.0 software.^[29] Additionally, the data were visualized with vmd,^[30] using a color code based on $\text{sign}(\lambda_2) \cdot \rho$ [–1.5 (blue), 0 (green), +1.5 (red)]. The required wavefunctions were obtained with PBE0/def2-TZVP.

Theoretical Evaluation of the Binding Constants

The above-described workflow allows to obtain the structures and energies of a small representative of the most likely ensemble of both, the hosts and the complexes. By that the possible error of taking the less probable (not lowest lying) conformer(s) into account is reduced. Additionally, by utilizing

the Boltzmann weighted energies of the lowest lying conformers, representing 99% of the total energy, mimic the conformational reality of the system even further. In Table 2 and Figure S18 (Supporting Information) the thus obtained calculated association energies are displayed. These energies were determined by the Gibbs free energy of the complex, subtracted with the Gibbs free energies of the host and the guest. In general, the binding is slightly overestimated, which is known for such complexes.^[6,31,32]

The non-corrected basis set superposition error (BSSE) can be taken into account as an additional factor. For all investigated CPPs, the overbinding is stronger for the C₇₀ complex than the C₆₀ ones. This circumstance originates from the calculated binding energy, which is in three of four cases higher for C₇₀ than for the corresponding C₆₀ complex.

Theoretical Evaluation of the Geometries and Non-covalent Interactions

For the discussion of the non-covalent interactions occurring within the investigated supramolecular complexes, the most abundant conformer (MAC) was utilized for the visualization of intermolecular forces. Within the ensemble of the diethyl phthalane CPP **2**, only conformers with the ether moiety facing inside the cavity were observed. This is in agreement with the crystal structure of the diethyl phthalane incorporated [8]CPP reported earlier by our group.^[33] The fact that the ether moiety is facing inside – in both cases, the CPP and its complexes – is further supported by ¹H-NMR spectroscopy of the 2@C₆₀ complex (Supporting Information, Figure S13). The optimized geometries of **3** and **4** show that the substituents tend to face out of the nanohoop, minimizing the repulsive interactions which is in agreement with the solid state structure of CPP **3** which we presented earlier.^[12]

The NCI plots of the MAC of the four investigated CPPs with the fullerenes are displayed in Figure 5. The parent [10]CPP complexes, show the π - π interactions which are expected to be present in the backbone of the substituted nanohoop as well. In both complexes a large interaction surface can be observed between the nanohoop and the fullerene. As indicated by the green color the interactions are of a weak nature, displaying π - π van der Waals forces. The shape of the NCI plot is similar in both, the C₆₀ and the C₇₀ complex.

Host	Guest	$\Delta G_{\text{bind,calc}}$	$\Delta G_{\text{bind,measure}}$ kJ/mol	abs. deviation
1	C ₆₀	-49.18	-39.09	10.10
	C ₇₀	-50.82	-32.35	18.47
2	C ₆₀	-35.75	-28.88	6.87
	C ₇₀	-33.30	-26.10	7.20
3	C ₆₀	-51.32	-33.52	17.80
	C ₇₀	-52.22	-27.88	24.34
4	C ₆₀	-48.13	-28.58	19.54
	C ₇₀	-48.18	-26.28	21.90

For a better understanding of the interactions, NCI scatter-plots of the complexes were depicted. The corresponding graphs for [10]CPP complexes with C₆₀ and C₇₀ are displayed in Figure 4b. In these 2D plots, the reduced density gradient (RDG) is plotted against the density multiplied by the sign of the second hessian eigenvalue ($\text{sign}(\lambda_2) \cdot \rho$). Thus, spikes close to $\text{sign}(\lambda_2) \cdot \rho = 0$ display weak interactions. Both NCI scatter-plots of 1@C₆₀ and 1@C₇₀ have sharp spikes close to $\text{sign}(\lambda_2) \cdot \rho = 0$, originating from the π - π interactions, which qualitatively appear similar, while being slightly more expressed in the C₇₀ complex (green circle) which resembles the more rough interactions in the NCI plot.

Additional interactions can be observed for the complexes of CPP **2**. As the lone pair of the oxygen is facing to the π -surface of the fullerene, strong attractive interactions can be observed, which are indicated by the blue color in the NCI plot. These additional interactions are similar for both complexes (C₆₀ and C₇₀). The scatter-plots of both reveal weak interactions close to $\text{sign}(\lambda_2) \cdot \rho = 0$. Comparing the data of the C₆₀ and the C₇₀ complex of CPP **2** a stronger interaction can be observed for the C₇₀ complex recognizable by the more intense spikes in the scatter plot (green bar). The C₆₀ and C₇₀ complexes of the CPPs **3** and **4** with their *tert*-butyl esters can form CH- π van der Waals interactions between the *tert*-butyl groups and the guests. In the C₆₀ complexes of CPPs **3** and **4**, only the belt-like NCI surface can be observed between the host and the guest which are the result of the concave-convex π - π interaction. Other attractive interactions between the substituents on the nanohoop and the fullerene guest cannot be observed. However, extending the π -surface of the fullerene – by changing from C₆₀ to C₇₀ – a new NCI surface emerges between the *tert*-butyl substituents of the nanohoop **3** and the egg-shaped fullerene. With a H_{substituent}-C₇₀ distance of ~ 3.8 Å these interactions are in the range of London dispersion forces. The increased number of weak interactions is also represented in the corresponding scatter-plots. Two new spikes appear at very low ρ values (green bar), while the blurry spike at -0.01 is approaching the RDG=0 line (green circle). This finding supports our interpretation of C₇₀ behaving like a π -extended C₆₀ in these supramolecular complexes. Interestingly, in none of the observed conformer of 3@C₇₀ both *tert*-butyl groups are facing toward the fullerene core, indicating that sterics and/or dipole moment outnumbers the potential additional London dispersion forces. In case of the more substituted CPP **4** the complexation of C₇₀ also induces an additional non-covalent interaction between the *tert*-butyl substituents and the fullerene compared to C₆₀, represented by a light green NCI surface. Surprisingly, only one out of four substituents interacts with the encapsulated fullerene in the MAC.

The insight obtained from the NCI plots and their scatter-plots support our assumptions originating from the experimental data: In all substituted cases the weak interactions are more pronounced for the C₇₀ complexes in comparison to the corresponding C₆₀ complex visualized by the scatter-plots. This effect appears to be stronger for the substituted nanohoops than for the parent [10]CPP, explaining the stronger beneficial substitution effect for the substituted nanohoops, described by

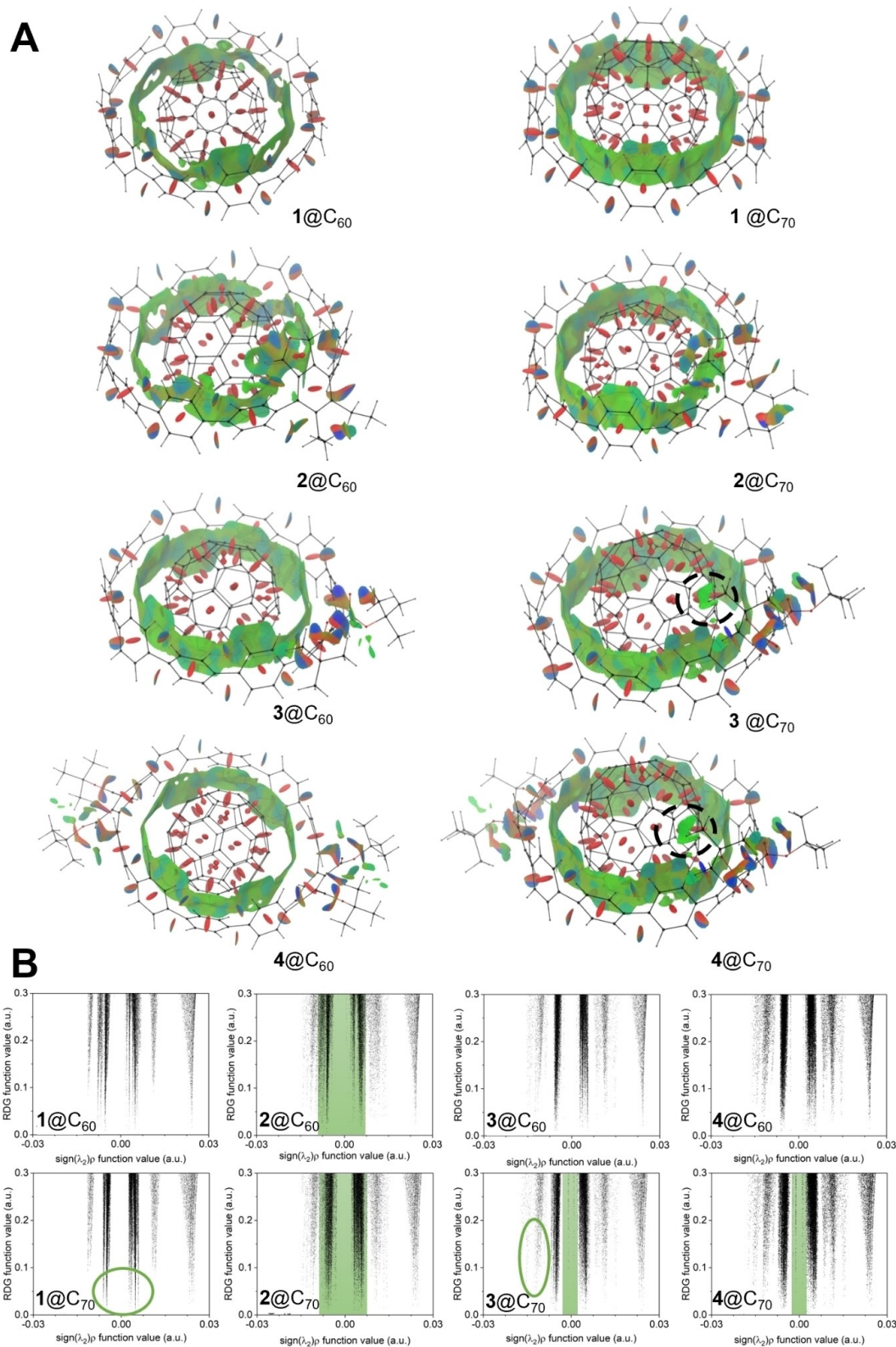


Figure 5. Calculated structures of the MAC of each complex with the isosurface displaying noncovalent interactions (A). Scatter plot (RDG function value vs. $\text{sign}(\lambda_2)\rho$ function value) of the noncovalent interactions of each in A shown complex (B).

the lower relative association energy (Figure 4, purple bar). In the visualized NCI plots the additional interactions with C₇₀ are

visible for the *tert*-butyl ester functionalized CPPs 3 and 4 while they are not as obvious in case of CPP 2 as in the C₆₀ complex

already attractive substituent fullerene interactions can be observed.

Conclusions

In summary, we presented a comprehensive host-guest study of substituted [10]CPPs with the fullerenes C₆₀ and C₇₀ investigating the association and interactions experimentally, as well as theoretically. With the method of fluorescence quenching the association energies of the complexes could be determined even though the differences are small. The observed trend shows an attractive substituent-fullerene interaction with regard to the ellipsoid fullerene C₇₀, which bears additional π -surface for attractive van der Waals forces. Additionally, the experimental data reveal, that the nature of the substituent has a comparable low impact, in contrast to the degree of substitution. The theoretical investigation was based on the whole ensemble of conformers utilizing the tools CREST and CENSO to obtain reliable structures and energies. Even though, the calculated energies overestimate the binding, these values perform well with respect to the literature cases of [10] and [11]CPP, which report an overbinding of one order of magnitude.^[6,31] Visualization and analysis of the noncovalent interactions support the assumptions based on the observed trends by qualitative comparison of the NCI plots. Interactions of the substituents with the encapsulated fullerene – especially in case of C₇₀ – reveal the attractive nature of these additional stabilizing effects. The presented results contribute to the understanding of non-covalent interactions within supramolecular complexes and provide quantitative data to design supramolecular carbon structures utilizing non-covalent interactions.

Experimental Section

Materials: Fullerenes C₆₀ and C₇₀ were purchased from TCI. The four substituted and unsubstituted cycloparaphenylenes were previously synthesized and used without further treatment.^[11–13]

C₆₀: ¹³C NMR (151 MHz, C₆D₆) δ 143.3.

C₇₀: ¹³C NMR (151 MHz, CDCl₃) δ 150.7, 148.2, 147.4, 145.4, 130.9.

[10]CPP 1: ¹H NMR (400 MHz, CDCl₃) δ 7.56 (s, 40H), ¹³C NMR (101 MHz, CDCl₃) δ 138.3, 127.5.

Substituted CPP 2: ¹H NMR (400 MHz, CD₂Cl₂) δ 7.64–7.54 (m, 26H), 7.54–7.50 (m, 4H), 7.17–7.13 (m, 4H), 4.01 (s, 4H), 3.04 (q, ³J = 7.4 Hz, 4H), 1.24 (t, ³J = 7.4 Hz, 6H); ¹³C NMR (101 MHz, CD₂Cl₂): δ 140.1, 139.4, 139.3, 139.2, 138.8, 138.7, 138.6, 138.6, 138.5, 135.9, 130.6, 128.0, 127.9, 127.83, 127.76, 127.72, 127.66, 127.4, 74.6, 23.9, 17.0. Digits were added to show the difference in the chemical shift. HRMS (APCI): calc. for [C₆₆H₅₁O]⁺: [M + H]⁺ 859.3935, found 859.3933.

Substituted CPP 3: ¹H NMR (400 MHz, CDCl₃) δ 7.60–7.51 (m, 32H), 7.46–7.40 (m, 4H), 6.75 (s, 2H), 1.46 (s, 18H); ¹³C NMR (101 MHz, CDCl₃): δ 167.0, 139.6, 139.4, 138.9, 138.47, 138.45, 138.43, 138.31, 138.28, 134.44, 131.42, 130.12, 127.56, 127.53, 127.51, 126.8, 82.5, 28.02. Digits were added to show the difference in the chemical

shift. HRMS (ESI): calc. for [C₇₀H₅₆O₄ + Na]⁺: [M + Na]⁺ 983.4071, found 983.4072.

Substituted CPP 4: ¹H NMR (600 MHz, CD₂Cl₂): δ 7.61 (s, 16H), 7.59–7.55 (m, 8H), 7.47–7.43 (m, 8H), 6.84 (s, 4H), 1.45 (s, 36H); ¹³C NMR (151 MHz, CD₂Cl₂): δ 167.5, 140.3, 140.0, 139.7, 139.14, 139.09, 135.1, 132.1, 130.8, 128.23, 128.17, 127.6, 83.1, 28.4. Digits were added to show the difference in the chemical shift. HRMS (ESI): calc. for [C₈₀H₇₂O₈ + 2Na]²⁺: [M + 2Na]²⁺ 603.2505, found 603.2504.

Fluorescence Quenching Experiments: The fluorescence quenching experiments were performed with a FP-8300 fluorescence spectrometer from Jasco. Solvents for spectroscopy were purchased from Merck or Chemsolute (Uvasol® or HPLC quality). The samples were irradiated with a Xe-lamp. Excitation and emission bandwidth were set to 2.5 nm. The fluorescence was measured between 400 nm and 600 nm with a scan speed of 200 nm/min and a data interval of 0.2 nm. The response time was set to 0.5 sec. The titrations with parent [10]CPP were irradiated at 340 nm, with di- and tetra-*tert*-butyl ester substituted [10]CPP at 338 nm and with diethyl phthalane incorporated [10]CPP at 326 nm.

The association constants were determined by threefold titrations. For each titration a 10⁻⁶ M to 10⁻⁷ M solution of the CPP was prepared in toluene. These solutions were used as solvent for a 10⁻⁴ M to 10⁻⁶ M solution of the different fullerene guests. Starting with 1800 μ l of CPP solution the fullerene (in CPP) solution was added in portions of 15–100 μ l. After each step of addition, the solution was mixed thoroughly, and a fluorescence spectrum was measured.

For the determination of the association constant the fluorescence (in a.u.) at the maxima (one maximum in case of parent [10]CPP and two maxima in case of the substituted [10]CPPs) were used. The data were plotted with non-linear regression utilizing the online tool "Bindfit" by P. Thordarson.^[16] As error of the mean values the standard deviation was used.

Supporting Information

The authors have cited additional references within the Supporting Information.^[34]

Acknowledgements

The authors are grateful to Dennis Gerbig for computational support and the Justus Liebig University for financial support. Open Access funding enabled and organized by Projekt DEAL.

Conflict of Interests

The authors declare no conflict of interest.

Data Availability Statement

The data that support the findings of this study are available in the supplementary material of this article.

Keywords: host-guest systems · macrocycles · computational chemistry · substituent effects · noncovalent interactions

- [1] C. A. Hunter, J. K. M. Sanders, *J. Am. Chem. Soc.* **1990**, *112*, 5525–5534.
 [2] S. E. Wheeler, J. W. G. Bloom, *J. Phys. Chem. A* **2014**, *118*, 6133–6147.
 [3] E. Riedel, C. Janiak, *Anorganische Chemie*, De Gruyter, Berlin, **2022**, pp. 554–561.
 [4] S. E. Lewis, *Chem. Soc. Rev.* **2015**, *44*, 2221–2304.
 [5] a) R. Jasti, J. Bhattacharjee, J. B. Neaton, C. R. Bertozzi, *J. Am. Chem. Soc.* **2008**, *130*, 17646–17647; b) H. Takaba, H. Omachi, Y. Yamamoto, J. Bouffard, K. Itami, *Angew. Chem. Int. Ed.* **2009**, *48*, 6112–6116; c) S. Yamago, Y. Watanabe, T. Iwamoto, *Angew. Chem. Int. Ed.* **2010**, *122*, 769–771.
 [6] T. Iwamoto, Y. Watanabe, T. Sadahiro, T. Haino, S. Yamago, *Angew. Chem. Int. Ed.* **2011**, *50*, 8342–8344.
 [7] A. Stergiou, J. Rio, J. H. Griwatz, D. Arçon, H. A. Wegner, C. P. Ewels, N. Tagmatarchis, *Angew. Chem. Int. Ed.* **2019**, *58*, 17745–17750.
 [8] Y. Xu, R. Kaur, B. Wang, M. B. Minameyer, S. Gsänger, B. Meyer, T. Drewello, D. M. Guldi, M. von Delius, *J. Am. Chem. Soc.* **2018**, *140*, 13413–13420.
 [9] H. Ueno, T. Nishihara, Y. Segawa, K. Itami, *Angew. Chem. Int. Ed.* **2015**, *54*, 3707–3711.
 [10] J. Rio, S. Beeck, G. Rotas, S. Ahles, D. Jacquemin, N. Tagmatarchis, C. Ewels, H. A. Wegner, *Angew. Chem. Int. Ed.* **2018**, *57*, 6930–6934.
 [11] J. Volkmann, D. Kohrs, H. A. Wegner, *Chem. Eur. J.* **2023**, *29*, e202300268.
 [12] D. Kohrs, J. Becker, H. A. Wegner, *Chem. Eur. J.* **2022**, *28*, e202104239.
 [13] J. Volkmann, D. Kohrs, F. Bernt, H. A. Wegner, *Eur. J. Org. Chem.* **2022**, e202101357.
 [14] D. Kohrs, J. Volkmann, H. A. Wegner, *Chem. Commun.* **2022**, *58*, 7483–7494.
 [15] E. R. Darzi, T. J. Sisto, R. Jasti, *J. Org. Chem.* **2012**, *77*, 6624–6628.
 [16] a) <http://supramolecular.org>; b) D. Brynn Hibbert, P. Thordarson, *Chem. Commun.* **2016**, *52*, 12792–12805; c) P. Thordarson, *Chem. Soc. Rev.* **2011**, *40*, 1305–1323.
 [17] a) F. Neese, *WIREs Comput. Mol. Sci.* **2012**, *2*, 73–78; b) F. Neese, *WIREs Comput. Mol. Sci.* **2022**, *12*, e1606.
 [18] C. Adamo, V. Barone, *J. Chem. Phys.* **1999**, *110*, 6158–6170.
 [19] F. Weigend, R. Ahlrichs, *Phys. Chem. Chem. Phys.* **2005**, *7*, 3297–3305.
 [20] B. Helmich-Paris, B. de Souza, F. Neese, R. Izsák, *J. Chem. Phys.* **2021**, *155*, 104109.
 [21] F. Weigend, *Phys. Chem. Chem. Phys.* **2006**, *8*, 1057–1065.
 [22] P. Pracht, F. Bohle, S. Grimme, *Phys. Chem. Chem. Phys.* **2020**, *22*, 7169–7192.
 [23] S. Grimme, F. Bohle, A. Hansen, P. Pracht, S. Spicher, M. Stahn, *J. Phys. Chem. A* **2021**, *125*, 4039–4054.
 [24] a) S. Grimme, A. Hansen, S. Ehlert, J.-M. Mewes, *J. Chem. Phys.* **2021**, *154*, 64103; b) J. W. Furness, A. D. Kaplan, J. Ning, J. P. Perdew, J. Sun, *J. Chem. Phys. Lett.* **2020**, *11*, 8208–8215.
 [25] A. V. Marenich, C. J. Cramer, D. G. Truhlar, *J. Phys. Chem. B* **2009**, *113*, 6378–6396.
 [26] S. Spicher, S. Grimme, *J. Chem. Theory Comput.* **2021**, *17*, 1701–1714.
 [27] C. Bannwarth, E. Caldeweyher, S. Ehlert, A. Hansen, P. Pracht, J. Seibert, S. Spicher, S. Grimme, *WIREs Comput. Mol. Sci.* **2021**, *11*, e1493.
 [28] E. Caldeweyher, S. Ehlert, A. Hansen, H. Neugebauer, S. Spicher, C. Bannwarth, S. Grimme, *J. Chem. Phys.* **2019**, *150*, 154122.
 [29] E. R. Johnson, S. Keinan, P. Mori-Sánchez, J. Contreras-García, A. J. Cohen, W. Yang, *J. Am. Chem. Soc.* **2010**, *132*, 6498–6506.
 [30] W. Humphrey, A. Dalke, K. Schulten, *J. Mol. Graphics* **1996**, *14*, 33–38.
 [31] T. Iwamoto, Y. Watanabe, H. Takaya, T. Haino, N. Yasuda, S. Yamago, *Chem. Eur. J.* **2013**, *19*, 14061–14068.
 [32] J. Antony, R. Sure, S. Grimme, *Chem. Commun.* **2015**, *51*, 1764–1774.
 [33] A.-F. Tran-Van, H. A. Wegner, *Beilstein J. Nanotechnol.* **2014**, *5*, 1320–1333.
 [34] a) J. G. Brandenburg, C. Bannwarth, A. Hansen, S. Grimme, *J. Chem. Phys.* **2018**, *148*, 64104; b) S. Ehlert, M. Stahn, S. Spicher, S. Grimme, *J. Chem. Theory Comput.* **2021**, *17*, 4250–4261; c) M. Bursch, J.-M. Mewes, A. Hansen, S. Grimme, *Angew. Chem. Int. Ed.* **2022**, *61*, e202205735.

Manuscript received: June 14, 2023
 Revised manuscript received: June 20, 2023
 Accepted manuscript online: June 21, 2023